

Dynamics of a Mobile Mechanical System with Vibration Propulsion (VibroBot)

Ivan A. Loukanov¹, Venko G. Vitliemov² Ivelin V. Ivanov²

¹Department of Mechanical Engineering, University of Botswana, Gaborone, Botswana

²Department of Technical Mechanics, University of Ruse, Ruse, Bulgaria

ABSTRACT: *In this study the mathematical model of unidirectionally moving prototype of a mobile mechanical system with vibration propulsion (VibroBot) is proposed and investigated. The results of a numerical experiment with the data of a real prototype having non-linear elastic and dissipative characteristics are presented. The effects of the variation of parameters of the model on the dynamics of the VibroBot are studied and analyzed. The requirements for mechanical improvements of the propulsion system are defined based on the results of physical experiments previously accomplished. It was found that the mean robot velocity is very sensitive upon most of the parameters of the mechanical system. Also the proposed mathematical model visualizes how the energy of the rearward stroke of propulsion mechanism can be transformed into an increased mean velocity of the forward motion.*

Keywords: *mathematical model, numerical experiment, vibrobot, vibration propulsion, robot dynamics.*

I. INTRODUCTION

Mobile robots with vibration propulsion known as Vibrobots are subject of increased interest. It is inspired by some of their properties when moving under different conditions, under the requirements for energy efficiency, small size and to be ecologically friendly. The Vibrobots have a simple design, do not require complex transmission mechanisms and achieve high degree of adaptability. Their distinctive features are that they operate in the vicinity of the main resonance and have dynamic non-linearity, which obstructs their study.

The Vibrobots are propelled as a result of the action of inertia forces generated by the relative motion of internally rotating unbalanced masses in the propulsion system and the external friction forces. Most studies conducted with different Vibrobots are related to analytical modeling, experimental prototype testing and computer simulation of their dynamic behavior [1], [2], [3], [4], [5].

It is known that vibration-operating machines are more effective than non-vibration machines when tuned to resonance regimes [6]. In these cases the non-stationary internal ties in the mechanical system are the causes for high sensitivity, parametric oscillations and generation of oscillations with large amplitudes in some elements. In this case, conditions for violation of the dynamic strength are created as in number of cases periodic jumping motions with separation from the supporting surfaces are detected.

In this study a mathematical model of a VibroBot with one-way motion is created, based on experimental data obtained in [7] for a prototype model studied in [8], [9]. With the aid of numerical experiment a dynamic analysis of this model is conducted and the conditions for the dynamic improvement are found.

II. MATHEMATICAL MODEL

In Fig. 1 the physical model of a VibroBot is shown. The rotating motion of the unbalanced counter-rotating masses is converted into a one-way pulsating motion of the propulsion mechanism and the chassis. The unidirectional motion is achieved by means of one-way roller bearings built into the wheel's hubs that allow rotation motion in one direction and block the rotation of the wheels in the opposite direction.

For the creation of a mathematical model of the prototype model shown in Fig. 1 we consider a 5-mass 2D-model of the three-dimensional 8-mass mechanical system illustrated in Fig. 2. We assume that all masses of this model are distributed in plane shapes that move in a vertical plane, matching the reference XOZ plane of the introduced absolute coordinate system $OXYZ$ (Fig. 2). In the direction of the axis OY the spatial mechanical system has a dynamic symmetry. This assumption is true about the excitation effect of the two counter-rotating unbalanced masses $m_3/2$ and for the symmetrically positioned elastic and dissipative ties, but is approximate for the location of mass centers of the individual bodies.

The bodies 1 and 2 of weights G_1 and G_2 perform rectilinear-translation motions. The excitation action of the two counter-rotating unbalanced masses $m_3/2$ is directed along the OX axis. This effect can be simulated by means of the periodic motion of the equivalent body 3 relative to body 2, considered to be a point mass of weight $G_3 = m_3g$, that moves in accordance of a harmonic periodic law $\eta(t)$.

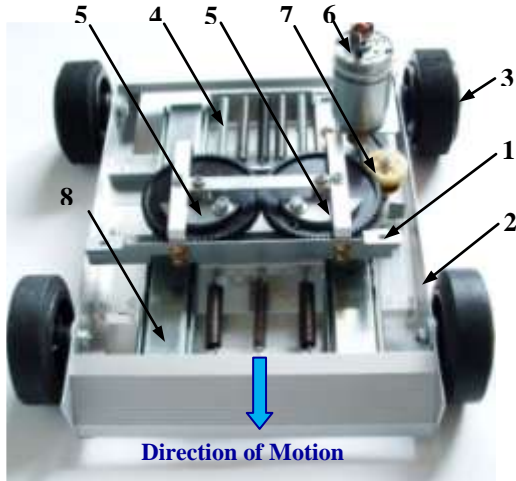


Fig. 1 shows the prototype of vibrobot, where: 1 – is the shaker, 2 –chassis, 3 –wheels & one-way bearings, 4- springs, 5- wheels & one-way bearings. 6- motor. 7- gears. 8- linear bearings.

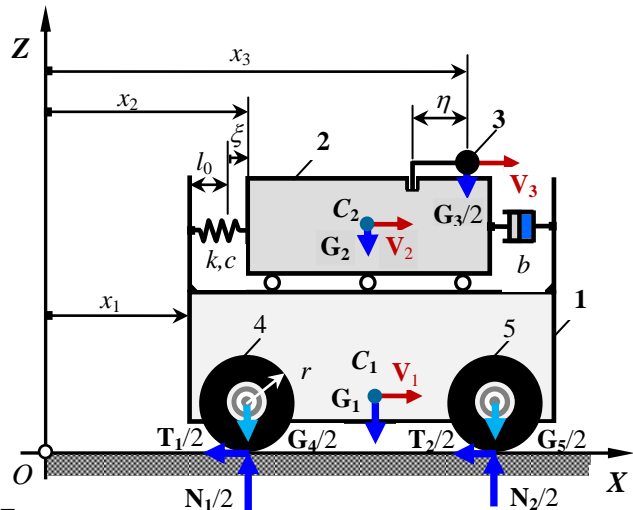


Fig. 2 presents the dynamic model of the

We introduce the generalized coordinates x_1, x_2, x_3 , that define the position of the bodies 1, 2 and 3 within the XOZ coordinate plane (Fig. 2).

The coordinates x_1, x_2 and x_3 are inter-connected through the equations:

$$(1) \quad \begin{aligned} x_2(t) &= x_1(t) + l_0 + \xi(t), \\ x_3(t) &= x_2(t) + l_2 + \eta(t), \end{aligned}$$

where: ξ is the measure of the relative variation of the length of the equivalent spring to its initial static state; $\eta(t) = \rho \sin(\omega t + \phi_0)$ – is the law of periodic motion of body 3; the distance l_0 is the initial length of the equivalent spring; distances l_2, ρ , the initial phase angle ϕ_0 of the rotating unbalanced masses and the angular velocity ω are assumed constant quantities. The wheels of the robot, modeled as solid (equal in pairs) bodies 4 and 5 are performing general plane motions. Their mass centers have velocities equal to the velocity $V_1 \equiv dx_1/dt$ of body 1, because their axes are fixed to it and are pushed directly by that body (Fig. 1).

We present the following designations for the absolute accelerations of the bodies of the mechanical system in consideration as:

$$(2) \quad \begin{aligned} a_1 &\equiv d^2x_1/dt^2 \equiv dV_1/dt, \\ a_2 &\equiv d^2x_2/dt^2 \equiv dV_2/dt, \\ a_3 &\equiv d^2x_3/dt^2 = a_2 + d^2\eta/dt^2 \equiv a_2 - \omega^2\rho\sin\psi \equiv a_2 - \omega^2\eta, \\ \varepsilon &= a_1/r, \end{aligned}$$

where: ε is the angular acceleration of the wheels under the assumption that they are rolling with no slip.

To derive the differential equations of motion by the method of kineto-statics [10], we split the mechanical system into the individual bodies and present the following forces:

- active forces $\mathbf{G}_i, i = 1, 2, \dots, 5$,
- reactions $\mathbf{N}_j, \mathbf{T}_j, j = 1, 2$,
- the forces of interaction between the bodies $\mathbf{R}_v, v = 1, 2, 3, \mathbf{F}_k$ and \mathbf{F}_b ,
- inertia forces $\square_l, l = 1, 2, \dots, 5$,
- the moments of inertia forces $\mathbf{M}_\delta^\Phi, \delta = 4, 5$,

where: $\mathbf{G}_i = m_i \mathbf{g}$ are the weights of the bodies; $F_k = -(k + c\xi^2)\xi, \xi = x_2 - (x_1 + l_0)$ is the measure of the equivalent elastic force \mathbf{F}_k with initial value $F_k(0) = [k + c(s_0 - l_0)^2](s_0 - l_0)$ with $s_0 \equiv x_2(0)$ and ξ is the dynamic deformation of the spring; $F_b = -b|V_2 - V_1|\sigma$ – is the measure of the resultant dissipative force \mathbf{F}_b , where $\sigma \equiv \text{sign}(V_2 - V_1)$ – is the signum-function; $F_f = -f(m_2 + m_3)g\sigma$ – is the measure of the friction force; $\square_l = -m_l \mathbf{a}_l$ – the D’Alambert’s inertia forces and $\mathbf{M}_\delta^\Phi = -(m_\delta r/2) a_1$ – the D’Alambert’s moments of the inertia forces.

Table 1 presents the free-body diagrams (FBD) of individual bodies of the VibroBot, where body 1 is the chassis, body 2 is the shaker, body 3 presents the rotating unbalanced masses and bodies 4 and 5 are wheels. Upon these bodies the active forces, reactions, forces of interaction between individual bodies and the components of inertia forces acting on each body are presented.

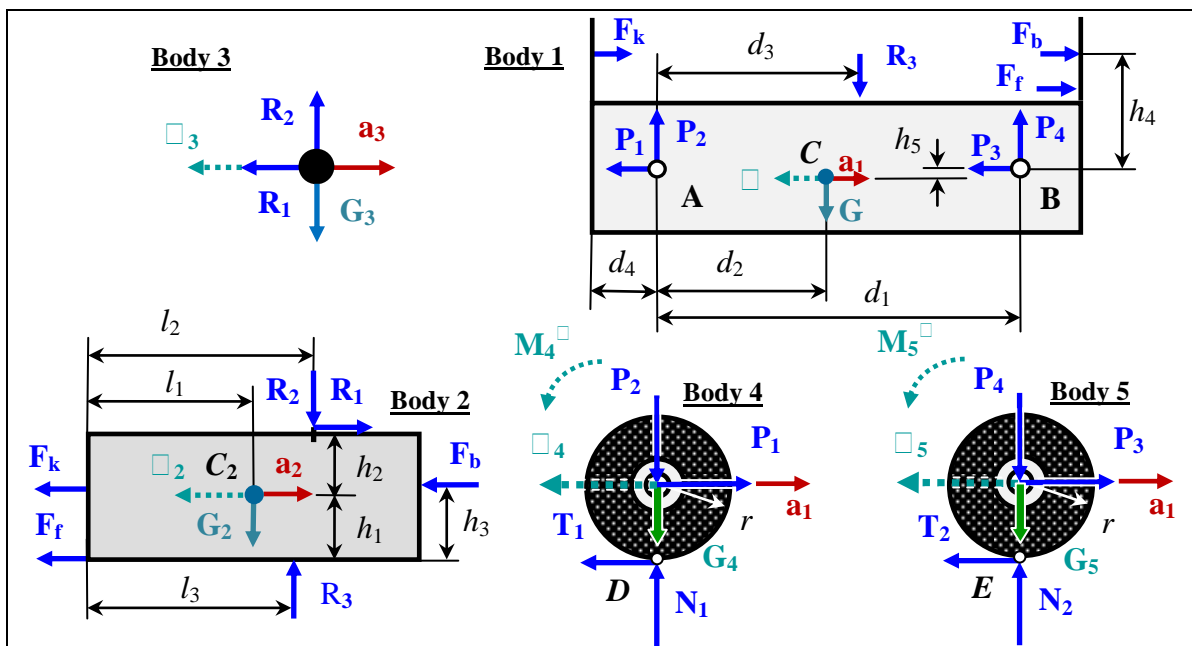
In accordance with the principle of D’Alambert’s these systems of forces are in equilibrium. The unknowns are the measures of the reactions $R_1, R_2, R_3, P_1, P_2, P_3, P_4, N_1, T_1, N_2, T_2$, the magnitudes of accelerations a_1, a_2, a_3 relevant to their originally selected directions as well as the unknown distance l_3 .

From the conditions of equilibrium (not shown) and (2) the above unknowns are found to be:

$$\begin{aligned}
 a_1 &= F_a / [m_1 + (3/2)(m_4 + m_5)] \\
 a_2 &= [m_3 \omega^2 \eta - F_a] / (m_2 + m_3) \\
 a_3 &= a_2 - \omega^2 \eta \\
 R_1 &= -m_3 a_3 \\
 R_2 &= m_3 g \\
 R_3 &= (m_2 + m_3) g \\
 P_1 &= (3/2) m_4 a_1 \\
 (3) \quad P_2 &= \{-F_a h_4 + [(m_2 + m_3)(d_1 - d_3) + m_1(d_1 - d_2)]g - m_1 a_1 h_5\} / d_1 \\
 T_1 &= (1/2) m_4 a_1 \\
 T_2 &= (1/2) m_5 a_1 \\
 P_3 &= (3/2) m_5 a_1 \\
 P_4 &= \{F_a h_4 + [(m_2 + m_3)d_3 + m_1 d_2]g + m_1 a_1 h_5\} / d_1 \\
 N_1 &= m_4 g + \{-F_a h_4 + [(m_2 + m_3)(d_1 - d_3) + m_1(d_1 - d_2)]g - m_1 a_1 h_5\} / d_1 \\
 N_2 &= m_5 g + \{F_a h_4 + [(m_2 + m_3)d_3 + m_1 d_2]g + m_1 a_1 h_5\} / d_1 \\
 l_3 &= l_1 + \{m_3 [g(l_2 - l_1) - a_3 h_2] - F_a (h_3 - h_1)\} / (m_2 + m_3) g
 \end{aligned}$$

where: $F_a = [k + c(x_2 - x_1 - l_0)^2](x_2 - x_1 - l_0) + [b|V_2 - V_1| + f(m_2 + m_3)g]\sigma$.

Table 1 Free body diagrams (FBD) of the individual bodies of the VibroBot



The differential equations and the initial conditions governing the motion of the mechanical system are:

$$\begin{aligned}
 dx_1/dt &= V_1, x_1(0) = 0 \\
 dV_1/dt &= [k + c(x_2 - x_1 - l_0)^2](x_2 - x_1 - l_0) + b|V_2 - V_1|\sigma + \\
 & f(m_2 + m_3)g\sigma / [m_1 + (3/2)(m_4 + m_5)], \quad V_1(0) = 0 \\
 (4) \quad dx_2/dt &= V_2, \quad x_2(0) = s_0 \\
 dV_2/dt &= m_3 \omega^2 \rho \sin(\omega t + \phi_0) - \{ [k + c(x_2 - x_1 - l_0)^2](x_2 - x_1 - l_0) + \\
 & b|V_2 - V_1|\sigma + f(m_2 + m_3)g\sigma \} / (m_2 + m_3), \quad V_2(0) = 0, \text{ where:} \\
 (5) \quad V_1 &= V_1(t), \text{ when } V_1(t) > 0, \text{ and } V_1 = 0, \text{ when } V_1(t) \leq 0
 \end{aligned}$$

The conditions (5) designate the one-way motion of the robot. They are realized by means of one-way roller bearings build into the hubs of wheels, which allow forward motion of the VibroBot whenever the driving inertia force acts in that direction and wedge the backward motion whenever the inertial force acts in the rearward direction.

Furthermore the equations (3), (4) and (5) are physically meaningful if at every instant $t \in [0, t_f]$ the condition (6) for continuous contact between the wheels and the ground is satisfied:

$$(6) \quad N_j^\circ = \min_t N_j(t) > 0, \quad j = 1, 2.$$

In the absence of slip of any wheel, the friction forces between the wheels and the ground are less than or equal to the maximum value of the resultant friction force T_j^* given by the equation:

$$(7) \quad T_j \leq T_j^* = \mu_0 N_j^\circ, \quad j = 1, 2$$

where: μ_0 is the static coefficient of friction. We also assume that when the motion of the VibroBot becomes stable, condition (7) is fully satisfied.

The mechanical perfection of the VibroBot design can be evaluated using a variety of criteria proposed by [11]. In general they can be combined into two groups – first to assess the mechanical means used in receiving a unit useful effect and second to characterize the intensity of dynamic regimes of operation.

The primary indicator for assessing the one-way VibroBot motion in a kinematic aspect is his average velocity given by the integral:

$$(8) \quad \langle V_1 \rangle = \frac{1}{t_f} \int_0^{t_f} V_1(t) dt,$$

where: $V_1(t)$ satisfies the condition (5).

As a local criterion for a dynamic intensity the ratio $K(t) = F_E(t)/F_D(t)$ of the applied horizontal resultant pushing force on the wheels $F_E(t) = \{P_1(t) + P_3(t)\}^+$ and that of the driving inertia force $F_D(t) = \{R_1(t)\}^+$ at the instants $t \in [0, t_f]$ for which $P_1(t) + P_3(t) > 0$ and $R_1(t) > 0$, is used.

$$(9) \quad \langle K \rangle = \langle F_E(t) \rangle / \langle F_D(t) \rangle,$$

Then for the evaluation of dynamic tension of the established motion of the VibroBot the average value of (9) is used as a local feature of $K(t)$ within the interval $t \in [0, t_f]$.

III. NUMERICAL EXPERIMENT

The mathematical model defined by (1)-(9) makes it possible to simulate the kinematic and dynamic features of the VibroBot as well as to analyze the influence of adjustable parameters of the prototype upon them.

A numerical experiment is carried out with nominal values of parameters of the prototype model substituted in (1)-(6) and determined in [7]. All these are listed in Table 2. For the numerical integration of differential equations (4) and (5) in the interval $t \in [0, t_f]$, the MATLAB-program “ode113” having relative accuracy of 10^{-6} and absolute precision of 10^{-8} is employed.

Table 2 presents the mechanical parameters of the VibroBot model

| Symbols | Value | Dimensions | Symbols | Value | Dimensions |
|----------------|--------------------|------------|-------------|-------------------|------------------|
| l_0 | 0.045 | m | ρ | 0.0125 | m |
| l_1 | 0.012 | m | r | 0.038 | m |
| l_2 | 0.040 | m | m_1 | 1.500 | kg |
| l_3 | calculated | m | m_2 | 1.165 | kg |
| $s_0 = x_2(0)$ | 0.060 | m | m_3 | 0.120 | kg |
| d_1 | 0.200 | m | m_4 | 0.240 | kg |
| d_2 | 0.099 | m | m_5 | 0.160 | kg |
| d_3 | $d_3 = l_3 + 0.06$ | m | ω | 40.19 | rad/s |
| d_4 | 0.050 | m | k | 2136 | N/m |
| h_1 | 0.035 | m | c | -43218 | N/m ⁴ |
| h_2 | 0.015 | m | b | 6.280 | Ns/m |
| h_3 | 0.014 | m | f | $1.729 (10)^{-4}$ | - |
| h_4 | 0.004 | m | φ_0 | 0 | deg |
| h_5 | 0.019 | m | t_f | 4 | s |

In Figs. 3 to 5 the simulated basic kinematic characteristics of the VibroBot are depicted: namely displacements, velocities and accelerations during the rectilinear motion of bodies 1, 2 and 3. The functions $x_1(t)$, $v_1(t)$ and $a_1(t)$ during a steady-state regime of motion of the VibroBot have a periodic nature of variation, which govern the robot pulsating motion. The sign variation of accelerations $a_1(t)$, $a_2(t)$ and $a_3(t)$ makes impossible the execution of a smooth variation of the acceleration $a_1(t)$, therefore the forward motion of the robot is a periodic pulsating motion.

The achievement of maximum possible asymmetry of the functions $a_3(t)$ and $a_1(t)$ is in principle feasible with the aid of a program controlled driving mechanism for a special class of wheeled robots – known as Inercoids [12]. These were invented, demonstrated and examined using the Newton laws by [12], where special experimental devices were designed and constructed to prove their feasibility and functionality. Although these devices exist and were proved working they are not accepted by the conservative scientific society, since according to them, they contradict the Newton laws of motion by propelling themselves without any contact with the ground. In this regard the invented, constructed and investigated VibroBot in this study does not defy the Newton's laws of motion as it uses friction forces between the wheels and the ground for its propulsion.

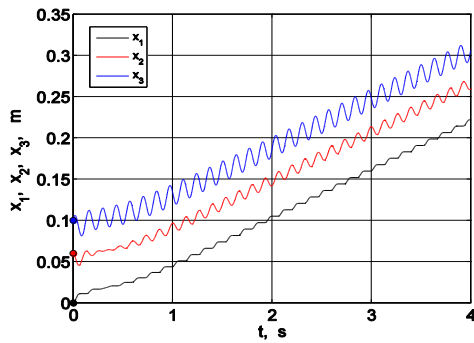


Fig.3 illustrates the displacements $x_1(t)$, $x_2(t)$ and $x_3(t)$ as functions of t

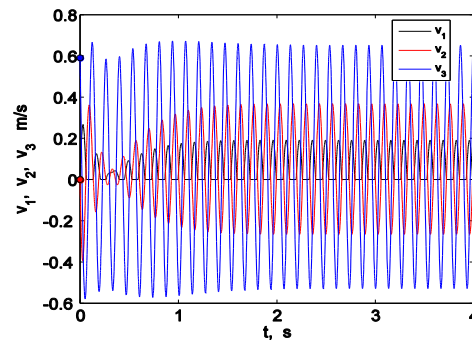


Fig. 4 shows the non-uniform variation of velocities $V_1(t)$, $V_2(t)$

The graph of the function $V_l(x_l)$ depicted in Fig. 6 illustrates an irregular state of alteration of the VibroBot phase condition during its accelerating motion.

It is seen that the horizontal components of reactions in the bearings of the wheels are changing in phase (Fig. 7) while the vertical reactions are varying out of phase. It is also indicated that the vertical load on the bearings of the rear wheels is greater than the load on the front ones (Fig. 8). The reason for this is that the mass center of the whole system is non-symmetrically located and is somewhat closer to the rear wheel axes but not in the middle of the wheel span as supposed to be. Similarly, to an accuracy of a constant, the components of reactions of the ground acting on the wheels are also variable (Fig. 9 and Fig. 10) and they follow the same style of action as those in figures 7 and 8.

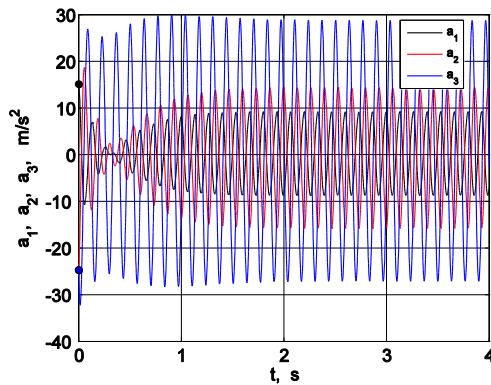


Fig. 5 indicates the variation of accelerations $a_1(t)$, $a_2(t)$ and $a_3(t)$

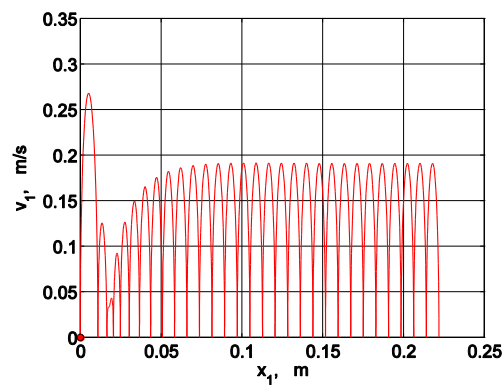


Fig. 6 shows the uneven change of the function $V_1(x_1)$ during the startup

Fig. 11 illustrate the variation of the predicted coefficients of frictions $\mu_1 = |T_1(t)/N_1(t)|$ and $\mu_2 = |T_2(t)/N_2(t)|$ to achieve rolling of the wheels without sliding. From this figure it is seen that both coefficient of frictions vary continuously during the motion of the VibroBot. With the help of the prototype of the VibroBot it is found experimentally [8] that for surfaces of different roughness and material properties the coefficient of static friction μ_0 takes values within the range [0.35, 0.75]. Therefore the significant difference between the actual and the predicted values of these coefficients will guarantee the non-slip motion of the wheels during the rearward stroke of the propulsion mechanism of the VibroBot. This is very important because if there is a sliding during this period there will be no forward motion of the robot at all and it will perform forth and back motion only corresponding to what the principle of linear momentum states. Or the mass center of the whole system will remain at the same position relevant to the reference plane OXY of the absolute OXYZ system.

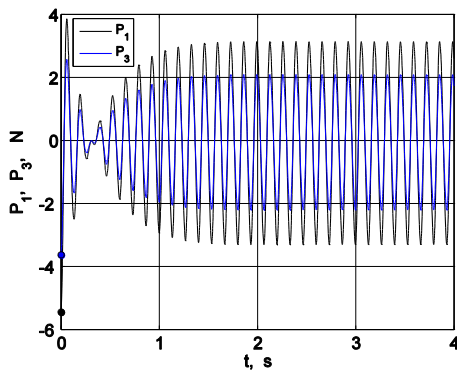


Fig. 7 shows the variation of horizontal forces P_1 and P_3 acting on the wheel axes

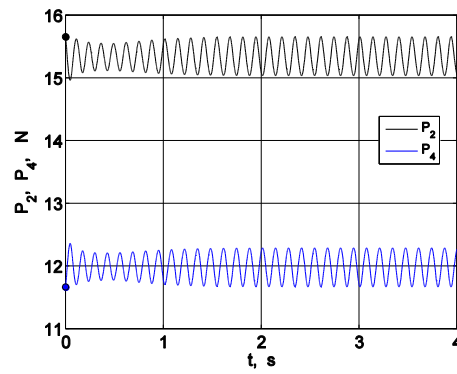


Fig. 8 presents the alternation of vertical forces acting on the wheel axes P_2 and P_4

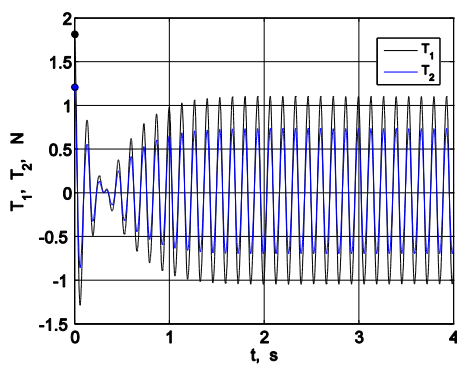


Fig. 9 demonstrates that friction forces $T_1(t)$ and $T_2(t)$ are varying in

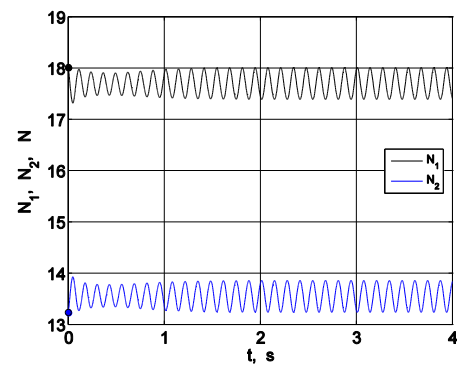


Fig 10 shows the normal reactions $N_1(t)$ and $N_2(t)$ varying out of phase

The influence of variation of prototype parameters within their ranges: $\phi_0 \in [0, 360]$ deg, $s_0 \in [0, 0.1]$ m, $\omega \in [30, 80]$ rad/s, $b \in [5, 25]$ Ns/m, $k \in [1000, 4000]$ N/m are next investigated to find their influences on the average velocity $\langle V_1 \rangle$. These can be traced out in Figs. 12, 13, 14, 15 as well as in Fig. 16.

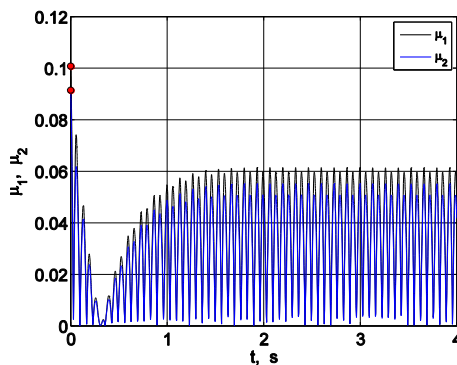


Fig. 11 shows the friction variables $\mu_1(t)$ and $\mu_2(t)$ acting on the wheels when in transition

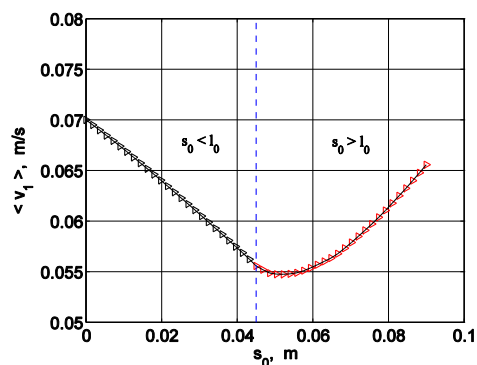


Fig. 12 illustrates the variation of $\langle V_1(s_0) \rangle$ in terms of initial spring pretension, s_0

From Fig. 12 we realize that the initial deformation of the equivalent spring has limited effect on the increase of the average velocity of motion of the Vibrobot. It is important that its value has to be larger than the expected resonance amplitudes of the propulsion mechanism for a preset frequency to prevent unhooking of tension springs from their sockets of attachment. If this occurs the motion of the Vibrobot will be ceased instantly and some damages of the propulsion mechanism may take place. This is because the amplitudes in resonance are very big as well as the magnitudes of inertia forces. The latter can induce strong impacts between the oscillating mechanism and other parts of the propulsion mechanism, hence possible damages.

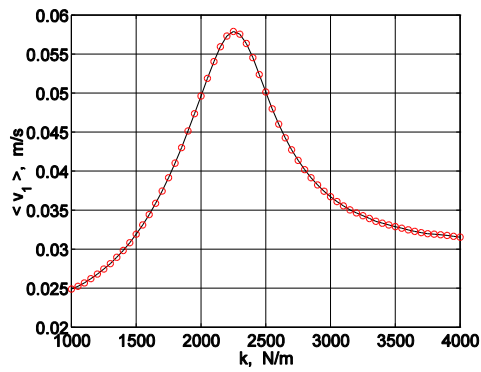


Fig. 13 explains the change of $\langle V_1(k) \rangle$ with variation of the spring stiffness

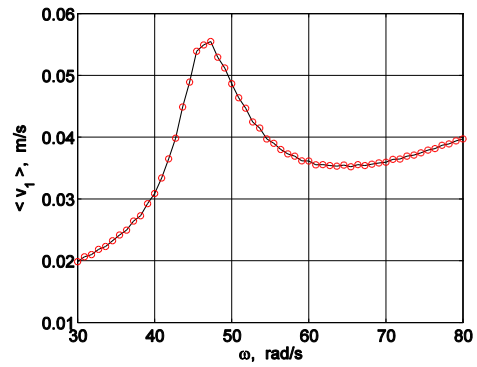


Fig. 14 presents the function $\langle V_1(\omega) \rangle$ in terms of increasing angular frequency

Fig. 13 and Fig. 14 justify the need for a coordinated choice of the values of parameters k and ω for proper functioning of the vibration propulsion mechanism in the area of the main resonance.

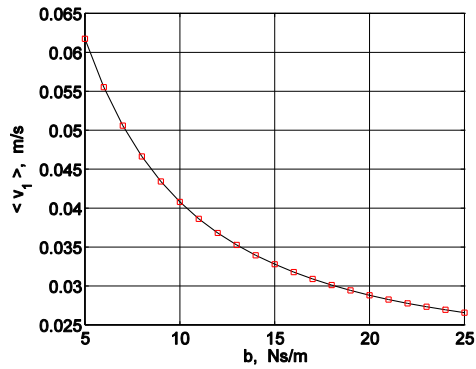


Fig. 15 shows the decrease of $\langle V_1(b) \rangle$ with increased damping, b .

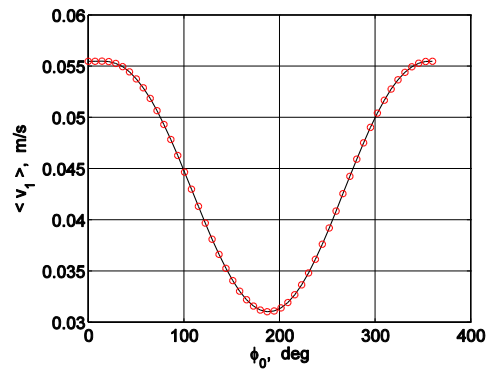


Fig. 16 illustrates the $\langle V_1(\phi_0) \rangle$ sensitivity from the phase

The non-linear nature of response of the function $\langle V_1(b) \rangle$ reveals the potential for an increase of the average velocity by reducing dissipation of energy in the propulsion mechanism. This is clearly seen in Fig. 15. That is way linear bearings were employed to guide and provide a support of the propulsion mechanism. That is way linear bearings were employed to guide and provide low friction in the propulsion mechanism.

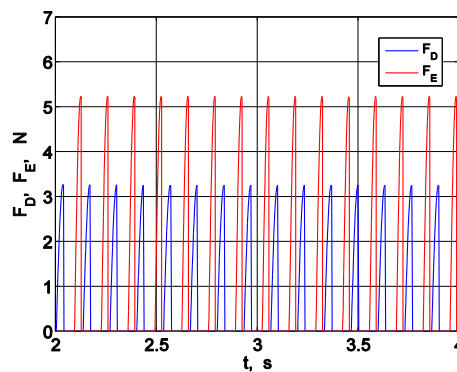


Fig. 17 presents the gap between $F_D(t)$ and $F_E(t)$ forces within $t \in [2, 4]$ s

Fig. 16 illustrates the specific feature of the vibration drive that $\langle V_1 \rangle$ is highly sensitive to the variation of the initial phase angle ϕ_0 of the rotating unbalanced masses at the beginning of the startup process. The preferred value of the phase angle should be as close as possible to zero at the beginning of motion in order to achieve high mean velocity corresponding to its maximum value, as seen in Fig. 16.

Fig. 17 shows the difference in magnitudes of the resultant horizontal propulsion force $F_E(t)$ acting on the wheels and the driving inertia force $F_D(t)$. The larger the difference between these forces the greater the

propulsion force but the higher the dynamic intensity will be. For the set interval $t \in [2, 4]$ s within the settled motion of the VibroBot the criterion for dynamic intensity (9) was calculated to have a value of $\langle K \rangle = 2.235$ indicating relatively high dynamic loading conditions. Generally, the larger the values of resonance frequency the higher the values of $\langle K \rangle$ are. This is due to the increased dynamic action of inertia forces generated at high frequencies of resonance because of very high values of the accelerations.

IV. CONCLUSIONS

The vibration propulsion is a non-traditional way to accomplish forward motion of wheeled robots. In this study the created non-linear model of a VibroBot with unidirectional motion is based upon experimental data of the force characteristics of a functional prototype model [7], [13]. The formulated mathematical model allows simulating and analyzing the specific features of the robot's motion and its kinematics and dynamics.

Numerical results reveal strong sensitivity of the mean velocity of the VibroBot to the change of the initial pretension of the equivalent spring (Fig. 12) and its stiffness (Fig. 13), to the variation of angular frequency (Fig. 14) up to 55-60 rad/s, to the dissipation of energy in the propulsion mechanism (Fig. 15) and to the value of the initial phase angle of the periodic rotation of unbalanced masses (Fig. 16). The passive nature of propulsion of the wheels provides with a large reserve meeting the condition of rolling without slipping on surfaces of different roughness and material properties (Fig. 11).

The resonance regime of vibration propulsion promises achieving maximum average velocity of motion but gives rise to high dynamic overloads on the propulsion mechanism and on all bearings. The potentials for mechanical improvement of the VibroBot design may be determined after solving the task of optimization synthesis, in which to the variable kinematic and dynamic parameters of the model to add masses of all bodies and some of the non-utilized distances. The results of this study will provide opportunity in optimizing the propulsion mechanism and improving the mean velocity of motion of the robot upon different soil conditions. Also this will help utilizing the energy of the backward stroke of the propulsion mechanism in improving the forward motion of the robot and increasing its mechanical efficiency. This can be achieved by storing part of the kinetic energy of the backward motion of the propulsion system into a system of springs and transform it later into a forward motion of the Vibrobot [6].

REFERENCES

- [1] Chernousko, F. Zimmermann, K. Bolotnik, S. Yatsun, I. Zeidis. Vibration-driven robots. *Workshop on Adaptive and Intelligent Robots: Present and Future*. Proceedings of the Institute for problems in Mechanics, Russian Academy of Science, Moscow, Vol. 1, 26–31, 2005.
- [2] Jatsun, S., N. Bolotnik, K. Zimmerman, I. Zeidis. Modeling of motion of vibrating robots. *12-th IFToMM World Congress, Besançon, France, June 18–21, 2007*.
- [3] Jatsun, S., V. Dyshenko, A. Yatsun, A. Malchikov. Modelling of robot's motion by use of vibration of internal masses. *Proceedings of EUCOMES 08, the Second European Conference on Mechanism Science*. M. Ceccarelli (Ed.), Springer, New York: 262–270, 2009.
- [4] Bolotnik, N., I. Zeidis, K. Zimmermann, S. Yatsun. Vibration-driven robots. *56th International Scientific Colloquium. Ilmenau University of Technology*, 2011.
- [5] Provatidis, C.G. Design of a propulsion cycle for endless sliding on friction ground using rotating masses. *Universal Journal of Mechanical Engineering*, Vol. 2, No. 2, 35–43, 2014.
- [6] Blekhman, I.I. *Vibrational Mechanics: Nonlinear dynamic effects, General approach, Applications*. World Scientific, Singapore, 2000.
- [7] Loukanov, I.A., V.G. Vitliemov, I.V Ivanov. Multi-criteria identification of vibrobot dynamic characteristics. To be published 2015, a
- [8] Loukanov, I.A. Using inertial forces as a source of forward motion, *Mechanics of Machines, Technical University Varna, Vol. 23 (110), No. 2*, 104–107, 2014, a.
- [9] Loukanov, I.A. Applications of inertial forces for generating unidirectional motion. *Proceedings of University of Rouse, Vol. 53, Book 2: Mechanics, Mechanical and Manufacturing Engineering*: 9–19, 2014, b.
- [10] Meriam, J.L., L.G. Kraige. *Engineering Mechanics*. Vol. 2. Dynamics, 7th ed., John Wiley & Sons, New York, 2012.
- [11] Gorskii, B.E. *Dynamic Improvement of Mechanical Systems*. Technics, Kiev, 1987 (in Russian).
- [12] Tolchin, V.N. *Inertoid. Inertia force as a source of motion*. Perm publishers, Perm, 1977 (in Russian).
- [13] Loukanov, I.A. Inertial propulsion of a mobile robot. *Journal of Mechanical & Civil Engineering, Vol.12, No.2, Ver.2*: 23–33, 2015, b